Published by :
http://www.ijert.org

International Journal of Engineering Research & Technology (IJERT)
ISSN: 2278-0181
Vol. 5 Issue 10, October-2016

Automated Classification of Tuberculosis by PSO based Machine Learning using Chest Radiographs

S. Pushparani.,
Assistant professor
Dept of Computer Science and Engineering,
Meenakshi college of Engineering, Chennai.

Dr. V. Vallinayagam. ,
Professor
Dept of Mathematics,
St Joseph's college of Engineering, Chennai.

Dr. A. Chandra Sekar,
Professor
Dept of Computer Science and Engineering,
St Joseph's college of Engineering, Chennai.

Dr. Jani Anbarasi,
Assistant professor
Dept of Computer Science and Engineering
Agni college of Engineering, Chennai.

***Abstract* - Classification of tuberculosis based on chest X-Rays is the most feasible and faster when compared with other alternate slow and unreliable methods like Sputum smear microscopy. This paper presents an automated method for identifying TB in chest radiographs. Initially the chest X-ray images are segmented by nature inspired multilevel PSO based segmentation method. From the segmented images textural feature vectors are calculated using gray-level co-occurrence matrix. This feature vector is used for classifying the chest X-rays into normal and abnormal using neural network classifier. Performance of this system is measured on the data set collected from various diagnostic centers in Chennai, India. 75% of the data set are used for training while25 % datas in the dataset is used for testing the classifier. The accuracy achieved is greater than 90% for each level of segmentation. The accuracy is compared with other existing systems**

Index Terms : Segmentation, multilevel PSO, Tuberculosis, Chest X-ray, feature vector, co-occurence matrix

I. INTRODUCTION

Classification is a supervised data mining task by which numerical datas can be classified according to their occurrence in the databases to build a model for prediction purpose. Several diseases like tuberculosis, pneumonia, lung cancer are affecting lungs immediately and their diagnosis through lung x-rays are faster and cheaper. Tuberculosis is the second leading infectious disease that causes a major threat in many regions of the world. 1.2 million people are affected throughout the world [1]. Diagnosing TB is always a major challenge because the identification using sputum smear microscopy is an ancient technique which was developed before 100 years. Several skin tests are also performed to determine whether an individual has contracted TB and is not reliable most of the time. An automated approach is proposed by Stephen Jaeger for identifying TB in chest X-rays (CXRs) [2-4] where X rays are chosen due to the low cost yet providing high yield. TB screening analysis is performed using datasets selected from Montgomery County (MC) dataset. In this paper discrimination of the normal and abnormal CXRs using Neural network based PSO segmentation process is proposed for the dataset collected from various diagnostic centers in India.

Digital chest radiography and digital image processing techniques, assists a lot in screening and diagnosing TB to a greater extent. Ginnekan et al. A survey states that there is no system to predict chest radiographs accurately [5-7]. Automated nodule detection is one of the best automation schemes for CXR and CT images. Computer aided diagnosis (CAD) systems have been evaluated by many researchers to identify the capability of commercially available systems to detect lung nodules [8-10]. CAD system successfully assists in diagnosing lung cancer nodules [11] however nodules refers only one of the many manifestations of TB in radiographs. Due to the complexity in developing a fully automated CAD system for X ray analysis, researchers have concentrated on finding a solution for few specific sub problems [12]. Segmentation of lungs is a major task required from the CAD system to evaluate CXR's. It is also needed to segment Ribs, heart and clavicles [13]. Dawoud [14] proposed an iterative based segmentation which combined intensity information with the shape priors trained over the publicly available JSRT database.

Ginneken et al [15] proposed a feature extraction which divided the lungs into various overlapping regions and extracted the features from each region. Abnormal signs are detected through the moments of response of a multiscale filter band. The left and the right lung field were used as different features whereas training was performed by voting and weighed integration process. Most of the papers on CAD did not specifically work for any particular diseases. Whereas only a few worked in identifying TB [15-18]. Hogeweg et al combined texture based abnormality detection with a clavicle detection stage in order to suppress false positive responses [16]. Similarly Hogeweg used a similar combination of pixel classifiers

International Journal of Engineering Research & Technology (IJERT)
ISSN: 2278-0181
Vol. 5 Issue 10, October-2016

and an active shape model for the clavicle segmentation. Freedman et al [20] showed that the performance can be increased by automatic suppression of ribs and clavicles in CXR's. Availability of the clavicle in upper lung zone strongly indicates that TB has developed to a highly infectious state. Bayesian approach was developed to identify these regions automatically [17]. Xu et al used model based template matching technique based on Hessian matrix [19] to identify the cavities in the upper lungs. Arzhaeva *et al* used dissimilarity-based classification to find the abnormalities in the CXR's[22]. Similarly Pangilinan *et al* [23] proposed a stepwise binary classification algorithm to reduce the false positives in TB detection.

II. METHOD

This section describes the methods how chest images are classified by implementing different processing steps using machine learning algorithms. The automated classification system segments the image into various clusters or segments using multilevel PSO segmentation. From the segmented image various textural features are computed. These features are fed into the pre trained binary neural network classifier. By using gradient based back propagation thresholds the classifier classifies Normal and abnormal lungs

A. Multi Level PSO Based Segmentation

Segmentation is classified as texture based, histogram thresholding based, clustering based and region based merging methods. PSO algorithm was proposed by Eberhart and Kennedy in 1995 which takes the advantage of the swarm intelligence concept in machine learning. The collective behavior of unsophisticated agents interacts locally with their environment which collects and creates a coherent global functional pattern.

The fitness function used to evaluate the particle success in every step. To model a swarm every *n* particle is assumed to have n moves in a multidimensional space according to position (x_t^n) and velocity (v_t^n) which are highly influenced on local best (x_t^n), neighborhood best (n_t^n) and global best (g_t^n) information where

$$v_{t+1}^n = wv_t^n + \rho_1 r_1(g_t^n - x_t^n) + \rho_2 r_2(x_t^n - x_t^n) + \rho_3 r_3(n_t^n - x_t^n)$$

$$x_{t+1}^n = x_t^n + v_{t+1}^n$$

The coefficient w is the weight assigned to the inertial influence and $\rho_1, \rho_{2,} \rho_3$ are the learning factors which is set to 1.5. Depending upon the application $\rho_1, \rho_{2,} \rho_3$ values can be set for best results. r_1, r_2, r_3 are random vectors which generally assign a random number between 0 and 1. During the beginning the particle velocities are set to zero and their position is randomly set within the boundaries of the search space. The search space depends upon the intensity levels where worst possible values are assigned to local neighborhood and global best and the other parameters are adjusted accordingly to the population size and stopping parameters. The Size of the population plays an important role to obtain a good solution with the time limit. Stopping criteria can be predefined as number of iterations based on the problem. PSO updates neighbor and global information which affects the velocity and consequent position of particles{24].

Multilevel thresholding segments images into several distinct regions. So this thresholding technique of PSO should be extended to the required no of segments . If there are m thresholds $1< th_1<th_2< th_3.....< th_m<256$ divides the original image into m+1 levels C_0 for [1, . . . , k_1], C_1 for [k_1 +1, . . . , k_2], . . . , and C_m for [k_m +1, . . . , L]. Then the fitness function can be calculated by the equation

$$\sigma_b^2 = \omega_0(\mu_0 - \mu_t)^2 + \omega_1(\mu_1 - \mu_t)^2 .....\omega_m(\mu_m - \mu_T)^2$$

Where σ_b^2 is defined as the between class variance of the thresholding levels. By this the image can be segmented into various levels

B. Feature Computation

Texture plays an important role to identify the characteristics of objects. Various textural features for chest images with different levels of segmentation is computed For each image 22 features are extracted for each levels of segmentation and totally 88 features[25-27] .Textural features were calculated based on gray level coocurence matrix of the segmented chest image.

Consider an image of size N_x and N_y (columns and rows) where the grey level appearing at each pixel can be quantized to N_g levels as

Let L_x = {1,2,..... N_x} be columns,
L_y={1,2,..... N_y} be rows
G_x={1,2,.....N_{y-1}} set of N_g quantized grey levels

$L_x \times L_y$ is the image pixels ordered by their row column designation. Image I can be represented as a function that assigns some gray level into each pixel as a pair of coordinates in $L_x \times L_y$; I :
where $L_x \times L_y \rightarrow G$

The texture content information is specified by the matrix of relative frequencies P_{ij} with two neighboring pixels which are separated by *d* that occurs on the image, one with gray level i and other with gray level j

Let P(i,j) be the (i,j)th entry in the normalized GLCM. The mean and standard deviations for the rows and columns of the matrix are given as

Mean row (μx)= $\sum_i \sum_j i \cdot p(i,j)$

Mean column (μy) = $\sum_i \sum_j j \cdot p(i,j)$

SD row (σx) = $\sum_i \sum_j (i - \mu_x)^2 \cdot p(i,j)$

SD column (σy) = $\sum_i \sum_j (j - \mu_y)^2 \cdot p(i,j)$

and the features calculated for each levels of segmented image are

International Journal of Engineering Research & Technology (IJERT)
ISSN: 2278-0181
Vol. 5 Issue 10, October-2016

1. Autocorrelation: = $\sum_i \sum_j (ij)p(i,j)$

2.Contrast = $\sum_{n=0}^{G-1} n^2 \{\sum_{i=1}^{G}\sum_{j=1}^{G} p(i,j)\}, |i-j| = n$

3.Correlation= $\sum_{i=1}^{G-1}\sum_{j=1}^{G-1} \frac{\{i \times j\} \times p(i,j) - \{\mu_x \times \mu_y\}}{\sigma_x \times \sigma_y}$

4. Cluster Prominence

$= \sum_{i=1}^{G-1}\sum_{j=1}^{G-1} \frac{\{i \times j\} \times p(i,j) - \{\mu_x \times \mu_y\}}{\sigma_x \times \sigma_y}$

5. Cluster Shade = $\sum_{i=0}^{G}\sum_{j=0}^{G} \{i, + j - \mu_x - \mu_y\}^3 \times p(i,j)$

6.Dissimilarity = $\sum_i \sum_j |i-j| p(i,j)$

7. Energy: = $\sum_i \sum_j p(i,j)^2$

8. Entropy= $\sum_{i=1}^{G}\sum_{j=1}^{G} p(i,j) \times \log(p(i,j))$

9. Homogeneity = $\sum_i \sum_j \frac{1}{1+(i-j)^2} p(i,j)$

10. Maximum probability = $\underset{ij}{MAX}\ p(i,j)$

11. Variance = $\sum_{i=0}^{G}\sum_{j=0}^{G} \{i-\mu\}^2 \times p(i,j)$

12. Sum average = $\sum_{i=0}^{2G-2} i p_{x+y}(i)$

13. Sum variance

$= \sum_{i=2}^{2N_g} (i - \sum_{i=0}^{2G-2} p_{x+y}(i) \log p_{x+y}(i)) p_{x+y}(i)$

14. Sum entropy $= -\sum_{i=0}^{2G-2} p_{x+y}(i) \log p_{x+y}(i)$

15. Difference variance = Variance of P_{x+y}

17.Difference entropy $= -\sum_{i=0}^{G-1} p_{x+y}(i) \log p_{x+y}(i)$

18. Information measure of correlation1

$= \frac{\sum_{i=1}^{G}\sum_{j=1}^{G} p(i,j) \times \log(p(i,j)) + \sum_i \sum_j p(i,j) \log\{p_x(i) p_y(j)\}}{\max\{HX, HY\}}$

HX and HY are entropies of px and py

19. Information measure of correlation2 =

$(1 - \exp[-2.0(\sum_i \sum_j p_x(i) p_y(j) \log\{p_x(i) p_y(j)\} - \sum_{i=1}^{G}\sum_{j=1}^{G} p(i,j) \times \log(p(i,j))])^{1/2}$

20. Inverse difference (INV) = $\sum \frac{C_{ij}}{1+|i-j|}$

21. Inverse difference normalized (INN) = $\sum_{i,j=1}^{G} \frac{c_{ij}}{1+|i-j|^2 / G^2}$

22. Inverse difference moment = $\sum_{i=1}^{G-1}\sum_{j=1}^{G-1} \frac{1}{1+(i-j)^2} p(i,j)$

C. Classification

Here the classification of normal and abnormal chest X-rays are classified by neural network based classifier which uses conjugate gradient back propagation algorithm. Neural networks are general nonlinear classifiers. Neural network is a set of nodes and a set of links. The nodes correspond to neurons and the links represent the connections and the data flow between neurons. Connections are quantified by weights, which are dynamically adjusted during training. During training, a set of training instances is given. Each training instance is typically described by a feature vector (called an input vector). It should be associated with a desired output, which is encoded as an another vector, called the desired output vector. The back-propagation training method uses the following technique [28]: given an input pattern to the network, its output is compared with the desired output, and a distance or error between them is calculated. Next, all relevant weights are adjusted in such a way that next time the same instance is processed, the real output is closer to the desired one, which means an error decrease. This process continues until a
minimum error is reached or until a given number of training epochs is completed. To evaluate whether the system can perform at an acceptable level, in terms of accuracy and efficiency, we used the 10-fold cross validation technique [29].

The Scaled Conjugate Gradient (SCG) algorithm [30] denotes the quadratic approximation to the error E in a neighborhood of a point w by:

$$E_{qw}(y) = E(w) + E'(w)^T y + \frac{1}{2} y^T E''(w) y$$

In order to determine the minimum to $E_{qw}(y)$the critical points for $E_{qw}(y)$ must be found. The critical points are the solution to the linear system defined by Moller

$$E'_{qw}(y) = E''(w)y + E'(w) = 0$$

SCG belongs to the class of Conjugate Gradient Methods, which show superlinear convergence on most problems. By using a step size scaling mechanism SCG avoids a time consuming line-search per learning iteration, which makes the algorithm faster than other second order algorithms.

D. System Implementation

This TB detection technique is programmed in MATLAB and a computer having an Intel core 2duo, TS 800 processor and 3 GB of memory. The proposed scheme is tested on the TB data sets collected from various diagnostic centers in Chennai, India.

International Journal of Engineering Research & Technology (IJERT)
ISSN: 2278-0181
Vol. 5 Issue 10, October-2016

III. EXPERIMENTAL RESULTS

The Chest X-ray (CXR's) datas were collected from various diagnostic centers in Chennai India., This part of the paper presents the results of multilevel PSO based segmentation method on normal and abnormal chest X rays, the features computed from each level of segmentation and the accuracy of neural network classifier, . Fig 1 illustrates the normal chest X-rays along with a histogram of the image. Similarly fig 2 shows the abnormal CXRs and its histogram.

A. Segmentation

PSO method is the parameterized method, so the initialization parameters should be choosen for fast convergence. The values are given in Table 1. PSO based optimization method is stochastic random population based, each of them runs 20 times and the fitness values are brought in Table 2. All fitness values are calculated for 2, 3, 4, 5 thresholds(higher between class variances). Fitness values vary with the number of thresholds.

Table 1. Initial parameters for PSO

Parameter	Values
Num of Iterations	8
Population	200
ρ1	1.5
ρ2	1.5
W	1.2
V_{max}	2
V_{min}	-2
X_{max}	255
X_{min}	0

Table 2. Fitness values of different levels

Test image	Thresholds	PSO
Normal CXR	2	1309.90
	3	1568.90
	4	1705.90
	5	1768.60
Abnormal CXR	2	2171.70
	3	2552.80
	4	2699.50
	5	2783.60

To visually compare the segmented results of PSO, the segmented images with various threshold levels are given in Fig. 3. As can be seen from the figure, images with higher level of segmentation have more detail than the other images..

Fig 1 illustrates the normal chest X-rays along with a histogram of the image. Similarly fig 2 shows the abnormal CXRs and its histogram.

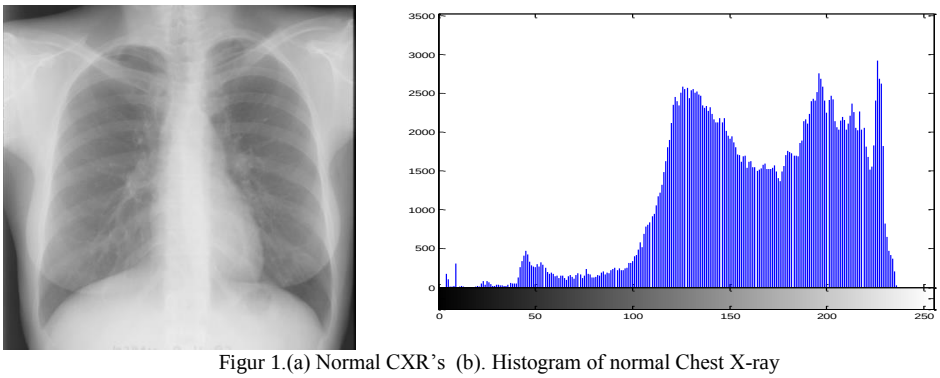

Figur 1.(a) Normal CXR's (b). Histogram of normal Chest X-ray

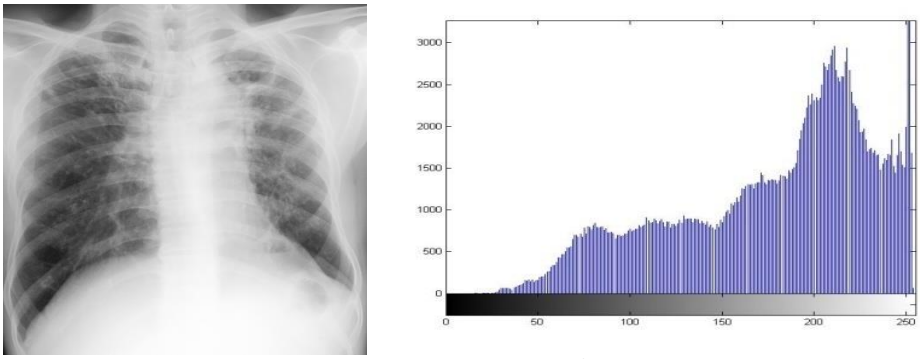

Figure 2.(a) abnormal Xray (b). histogram of abnormal Chest X-ray

International Journal of Engineering Research & Technology (IJERT)
ISSN: 2278-0181
Vol. 5 Issue 10, October-2016

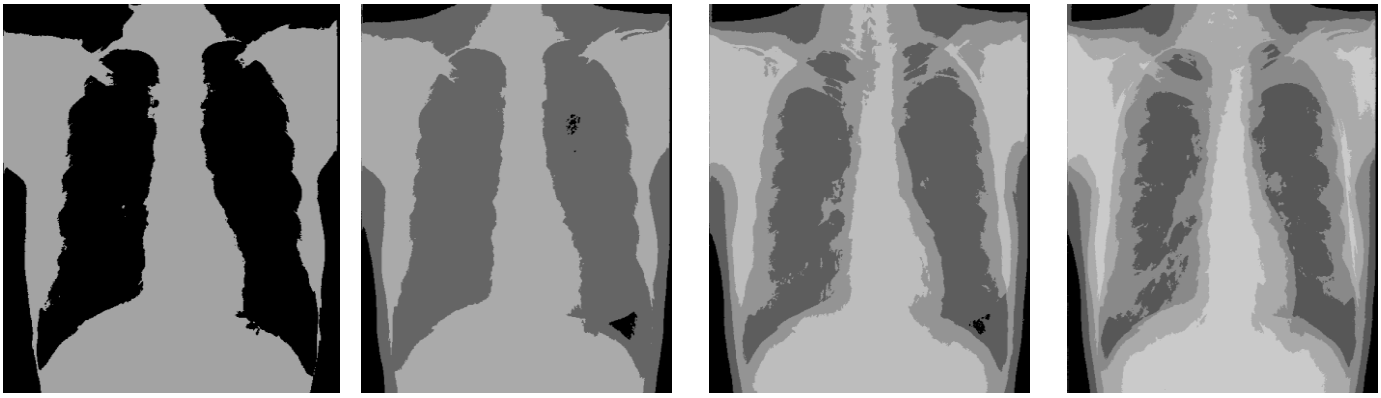

Figure.3 (a, b, c, d) segmented Normal images with 2, 3, 4, 5 thresholds

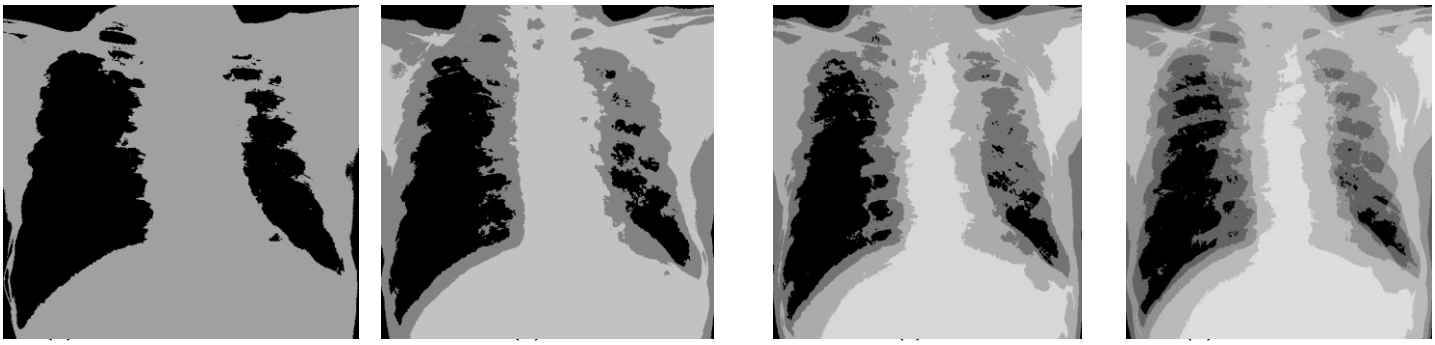

Figure.4 (a, b, c, d) segmented Abnormal images with 2, 3, 4, 5 thresholds

B. Classification

From the segmented images 22 textural features are extracted using Gray Level Co occurrence matrix of the each level of segmented CXR's. These textural features are extracted for 100 normal CXR's and 150 Abnormal CXR's. Based on the extracted features from CXR's the images were classified as Normal and abnormal images by the neural network Classifier. 75% of the datas are used for training the classifier and 25 % of the datas are used for testing the classifier Classification performance is determined using confusion matrix and ROC curve

The values tabulated are calculated as per the following equations from the corresponding confusion matrix to determine the performance of the classifier

$$\textbf{TP} = \sum_{i=1}^{p} predicted\,(normaldata)$$

$$\textbf{TN} = \sum_{i=1}^{q} [1 - predicted\,(abnormaldata)]$$

$$\textbf{FP} = \sum_{i=1}^{q} predicted\,(abnormaldata)$$

$$\textbf{FN} = \sum_{i=1}^{p} [1 - predicted\,(normaldata)]$$

$$\textbf{Sensitivity} = \frac{TP}{TP + FN}$$

$$\textbf{Specificity} = \frac{TN}{TN + FP}$$

$$\textbf{accuracy} = \frac{TP + TN}{P + N}$$

$$\textbf{Fscore} = \frac{2TP}{2TP + FP + FN}$$

$$\textbf{\textit{Matthews correlation coefficient}} = \frac{TP \times TN - FP \times FN}{\sqrt{(TP + FP)(TP + FN)(TN + FP)(TN + FN)}}$$

ROC curve summarizes the performance of a classifier over all possible thresholds. It is generated by plotting the True Positive Rate (y-axis) against the False Positive Rate (x-axis). The ROC curve shows different possible operating points depending on the confidence threshold for the neural network classifier. The area under the ROC curve (AUC) in Fig. is 95% with an overall classification accuracy of 93%. According to the ROC curve in Fig.5 Sensitivity of about 98% and false positive rate is slightly higher than 40% means specificity is a bit lower than 60%

The best validation performance is 0.061934 at epoch 37 of the neural network classifier with 22 inputs and 20 hidden neurons (Fig. 6)

International Journal of Engineering Research & Technology (IJERT)
ISSN: 2278-0181
Vol. 5 Issue 10, October-2016

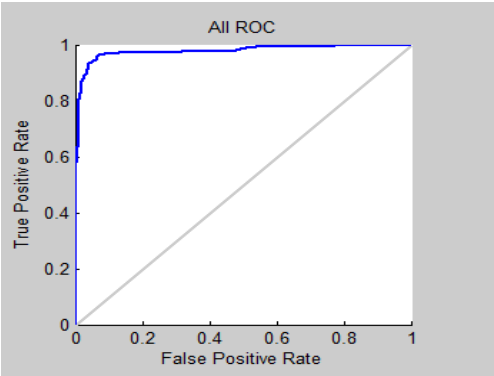

Fig 5. ROC CURVE

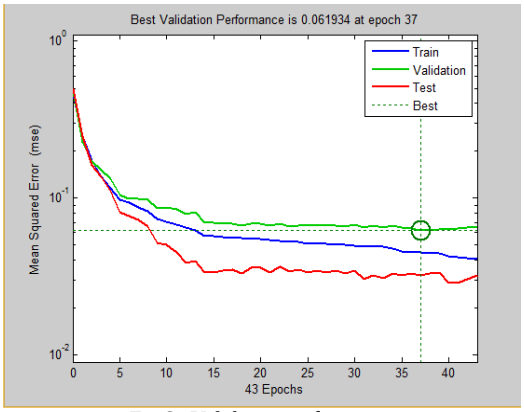

Fig 6. Validation performance

C. Comparison With Other Systems

The AUC value of this system is higher than the AUC values of the systems in [31] and [33]. Our AUC value is also slightly higher than the AUC value reported by Hogeweg *et al.*, who use a combination of texture and shape abnormality detectors [32].

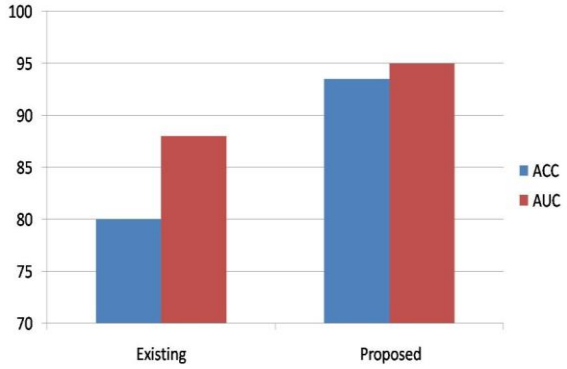

D. CONCLUSION

This paper proposed an automatic system that diagnoses the manifestation of TB. This scheme uses the features of PSO segmentation to effectively segment the lungs of the CXRs. The set of GLCM features are computed and are input to the neural network classifier which then classifies the given input image into normal and abnormal images. The results shows that an improved performance is achieved when compared to the existing. AUC and ACC values obtained are around 94% and 95% respectively. Also this work can to be extended using genetic algorithm to find the superior features that drive the solution. Also Comparison has to be performed with the human performance for the diagnosis system in future.

REFERENCES

[1] World Health Org., Global tuberculosis report 2012.
[2] S. Candemir, S. Jaeger, K. Palaniappan, S. Antani, and G. Thoma, "Graph-cut based automatic lung boundary detection in chest radiographs," in *Proc. IEEE Healthcare Technol. Conf.: Translat. Eng. Health Med.*, 2012, pp. 31–34.
[3] S. Candemir, K. Palaniappan, and Y. Akgul, "Multi-class regularization parameter learning for graph cut image segmentation," in *Proc.Int. Symp. Biomed. Imag.*, 2013, pp. 1473–1476.
[4] S. Jaeger, A. Karargyris, S. Antani, and G. Thoma, "Detecting tuberculosis in radiographs using combined lung masks," in *Proc. Int. Conf. IEEE Eng. Med. Biol. Soc.*, 2012, pp. 4978–4981.
[5] B. van Ginneken, L. Hogeweg, andM. Prokop, "Computer-aided diagnosis in chest radiography: Beyond nodules," *Eur. J. Radiol.*, vol. 72, no. 2, pp. 226–230, 2009.
[6] G. Lodwick, "Computer-aided diagnosis in radiology: A research plan," *Invest. Radiol.*, vol. 1, no. 1, p. 72, 1966.
[7] G. Lodwick, T. Keats, and J. Dorst, "The coding of Roentgen images for computer analysis as applied to lung cancer," *Radiology*, vol. 81, no. 2, p. 185, 1963.
[8] S. Sakai, H. Soeda, N. Takahashi, T. Okafuji, T. Yoshitake, H. Yabuuchi, I. Yoshino, K. Yamamoto, H. Honda, and K. Doi, "Computeraided nodule detection on digital chest radiography: Validation test on consecutive T1 cases of resectable lung cancer," *J. Digit. Imag.*, vol. 19, no. 4, pp. 376–382, 2006.
[9] J. Shiraishi, H. Abe, F. Li, R. Engelmann, H. MacMahon, and K. Doi, "Computer-aided diagnosis for the detection and classification of lung cancers on chest radiographs: ROC analysis of radiologists' performance," *Acad. Radiol.*, vol. 13, no. 8, pp. 995–1003, 2006.
[10] S. Kakeda, J. Moriya, H. Sato, T. Aoki, H. Watanabe, H. Nakata, N. Oda, S. Katsuragawa, K. Yamamoto, and K. Doi, "Improved detection of lung nodules on chest radiographs using a commercial computer- aided diagnosis system," *Am. J. Roentgenol.*, vol. 182, no. 2, pp.505–510, 2004.
[11] K. Doi, "Current status and future potential of computer-aided diagnosis inmedical imaging,"*Br. J. Radiol.*, vol. 78, no. 1, pp. 3–19, 2005.
[12] B. Van Ginneken, B. ter Haar Romeny, and M. Viergever, "Computeraided diagnosis in chest radiography: A survey," *IEEE Trans. Med. Imag.*, vol. 20, no. 12, pp. 1228–1241, Dec. 2001.
[13] B. Van Ginneken, M. Stegmann, and M. Loog, "Segmentation of anatomical structures in chest radiographs using supervised methods: A comparative study on a public database," *Med. Image Anal.*, vol. 10, no. 1, pp. 19–40, 2006.
[14] A. Dawoud, "Fusing shape information in lung segmentation in chest radiographs," *Image Anal. Recognit.*, pp. 70–78, 2010.
[15] B. van Ginneken, S. Katsuragawa, B. ter Haar Romeny, K. Doi, andM. Viergever, "Automatic detection of abnormalities in chest radiographs using local texture analysis," *IEEE Trans. Med. Imag.*, vol. 21, no. 2, pp. 139–149, Feb. 2002.
[16] L. Hogeweg, C. Mol, P. de Jong, R. Dawson, H. Ayles, and B. van Ginneken, "Fusion of local and global detection systems to detect tuberculosis in chest radiographs," in *Proc. MICCAI*, 2010, pp. 650–657.
[17] R. Shen, I. Cheng, and A. Basu, "A hybrid knowledge-guided detection technique for screening of infectious pulmonary tuberculosis from chest radiographs," *IEEE Trans. Biomed. Eng.*, vol. 57, no. 11, pp. 2646–2656, Nov. 2010.
[18] T. Xu, I. Cheng, andM.Mandal, "Automated cavity detection of infectious pulmonary tuberculosis in chest radiographs," in *Proc. Int. IEEE Eng. Med. Biol. Soc.*, 2011, pp. 5178–5181.
[19] L. Hogeweg, C. I. Sánchez, P. A. de Jong, P. Maduskar, and B. van Ginneken, "Clavicle segmentation in chest radiographs," *Med. Image Anal.*, vol. 16, no. 8, pp. 1490–1502, 2012.
[20] M. Freedman, S. Lo, J. Seibel, and C. Bromley, "Lung nodules: Improved detection with software that suppresses the rib and clavicle on chest radiographs," *Radiology*, vol. 260, no. 1, pp. 265–273, 2011.

International Journal of Engineering Research & Technology (IJERT)
ISSN: 2278-0181
Vol. 5 Issue 10, October-2016

[21] Kulkarni, R. V., & Venayagamoorthy, G. K. (2010). Bio-inspired algorithms for autonomous deployment and localization of sensor. IEEE Transactions on Systems, 40(6), 663–675

[22] Y. Arzhaeva, D. Tax, and B. Van Ginneken, "Dissimilarity-based classification in the absence of local ground truth: Application to the diagnostic interpretation of chest radiographs," *Pattern Recognit.*, vol. 42, no. 9, pp. 1768–1776, 2009.

[23] C. Pangilinan, A. Divekar, G. Coetzee, D. Clark, B. Fourie, F. Lure, and S.Kennedy, "Application of stepwise binary decision classification for reduction of false positives in tuberculosis detection from smeared slides," presented at the Int. Conf. Imag. Signal Process. Healthcare Technol., Washington, DC, 2011.

[24] Pedram Ghamisi, Micael S. Couceiro, Jón Atli Benediktsson & Nuno M.F.Ferreira. "An Efficient Method for Segmentation of Images Based on Fractional Calculus and Natural Selection", Expert Systems with Applications, Elsevier, 2012.

[25] R. M. Haralick, K. Shanmugam, and I. Dinstein, Textural Features ofImage Classification, IEEE Transactions on Systems, Man and Cybernetics, vol. SMC-3, no. 6, Nov. 1973

[26] L. Soh and C. Tsatsoulis, Texture Analysis of SAR Sea Ice Imagery Using Gray Level Co-Occurrence Matrices, IEEE Transactions on Geoscience and Remote Sensing, vol. 37, no. 2, March 1999.

[27] D A. Clausi, An analysis of co-occurrence texture statistics as a function of grey level quantization, Can. J. Remote Sensing, vol. 28, no. 1, pp. 45-62, 2002

[28] LiMin Fu, *Neural Networks in Computer Intelligence*, Ed-McGraw-Hill. 1994.

[29] Haykin, Simon S. *Neural Networks*: *A Comprehensive Foundation*. New York: Macmillan College Publishing Company, Inc., 1994.

[30] Moller, A *Scaled Conjugate Gradient Algorithm for Fast Supervised Learning*, Neural Networks, 6 (4), 1993, pp.525-533.

[31] B. van Ginneken, S. Katsuragawa, B. ter Haar Romeny, K. Doi, andM.Viergever, "Automatic detection of abnormalities in chest radiographs using local texture analysis," *IEEE Trans. Med. Imag.*, vol. 21, no. 2, pp. 139–149, Feb. 2002.

[32] L. Hogeweg, C. Mol, P. de Jong, R. Dawson, H. Ayles, and B. van Ginneken, "Fusion of local and global detection systems to detect tuberculosis in chest radiographs," in *Proc. MICCAI*, 2010, pp.650–657

[33] Y. Arzhaeva, D. Tax, and B. Van Ginneken, "Dissimilarity-based classification in the absence of local ground truth: Application to the diagnostic interpretation of chest radiographs," *Pattern Recognit.*, vol. 42, no. 9, pp. 1768–1776, 2009